

Electrochemical properties and durability of in-situ composite cathodes with  
 $\text{SmBa}_{0.5}\text{Sr}_{0.5}\text{Co}_2\text{O}_{5+\delta}$  for metal supported solid oxide fuel cells

John T. S. Irvine<sup>a</sup>, Joongmyeon Bae<sup>b</sup>, Jun-Young Park<sup>c</sup>, Won Seok Choi<sup>d</sup>,

Jung Hyun Kim<sup>e,\*</sup>

<sup>a</sup> School of Chemistry, University of St. Andrews, St. Andrews, Fife, KY16, 9ST, United Kingdom

<sup>b</sup> Department of Mechanical Engineering, Korea Advanced Institute of Science and Technology, 291 DaehakRo, Yuseong-Gu, Daejeon 305-701, Republic of Korea

<sup>c</sup> Hybrid Materials Center (HMC), Faculty of Nanotechnology and Advanced Materials Engineering, Sejong University, 209 Neungdong-Ro, Gwangjin-Gu, Seoul 143-747, Republic of Korea

<sup>d</sup> Department of Electrical Engineering, Hanbat National University, 125, Dongseo-Daero, Yuseong-Gu, Daejeon 305-719, Republic of Korea

<sup>e</sup> Department of Advanced Materials Science and Engineering, Hanbat National University, 125, Dongseo-Daero, Yuseong-Gu, Daejeon 305-719, Republic of Korea

Corresponding author:\*

Jung Hyun Kim: jhkim2011@hanbat.ac.kr, jhkim1870@gmail.com Tel: +82-42-821-1239, Fax: +82-42-821-1592, Department of Advanced Materials Science and Engineering, Hanbat National University, 125, Dongseo-Daero, Yuseong-Gu, Daejeon, 305-719, Republic of Korea

## **Abstract**

The electrochemical properties and long-term performance of an in-situ composite cathode comprised of  $\text{SmBa}_{0.5}\text{Sr}_{0.5}\text{Co}_2\text{O}_{5+\delta}$  (SBSCO) and  $\text{Ce}_{0.9}\text{Gd}_{0.1}\text{O}_{2-\delta}$  (CGO91) are investigated for metal supported solid oxide fuel cell (MS-SOFC) application.

The Area Specific Resistance (ASR) of an in-situ composite cathode comprised of 50 wt% of SBSCO and 50 wt% of CGO91 (SBSCO:50) is  $0.031 \Omega \text{ cm}^2$  in the first stage of measurement at  $700 \text{ }^\circ\text{C}$ ; this value of ASR increases to  $0.138 \Omega \text{ cm}^2$  after 1000 hours.

The ASR of SBSCO:50 (in-situ sample at  $750 \text{ }^\circ\text{C}$ ) is  $0.014 \Omega \text{ cm}^2$  at the initial stage of measurement; the increase of ASR after 1000 hours at  $750 \text{ }^\circ\text{C}$  is only  $0.067 \Omega \text{ cm}^2$ .

These results suggest that the optimum temperature for in-situ firing of an SBSCO:50 cathode sample of MS-SOFC is higher than  $700 \text{ }^\circ\text{C}$ , ideally around  $750 \text{ }^\circ\text{C}$ .

**Keywords:** Metal supported solid oxide fuel cell; Sr doped layered perovskite; Area specific resistance; In-situ cathode; Sintering effect

## 1. Introduction

Materials of layered perovskite type have recently been the subject of increased interest as cathode materials for Intermediate Temperature-operating Solid Oxide Fuel Cells (IT-SOFCs) because the high surface exchange coefficient and advanced bulk diffusion coefficient in layered perovskites result in a much higher performance than that observed for other materials used as conventional cathodes for IT-SOFCs [1-5].

Previous and on-going IT-SOFC cathode studies by our group have shown that Sr doped layered perovskite materials are promising cathode materials for application in SOFCs at temperatures between 500 °C and 700 °C [6-8]. Our research has been applied to layered perovskite compounds with the chemical formula  $\text{YBaCo}_2\text{O}_5$ , a material first synthesized and investigated in 1993 [6]. One very useful material in such layered perovskites is a 50% Sr-substituted oxide,  $\text{YBa}_{0.5}\text{Sr}_{0.5}\text{Co}_2\text{O}_{5+\delta}$ , which shows increased electrical conductivity, with a maximum value of  $130 \text{ S cm}^{-1}$  at 150 °C and a value of  $60 \text{ S cm}^{-1}$  at 700 °C; these values can be compared favorably to those of unsubstituted  $\text{YBaCo}_2\text{O}_{5+\delta}$ , which has a value of  $50 \text{ S cm}^{-1}$  as a maximum result at 300 °C and a value of  $20 \text{ S cm}^{-1}$  at 600 °C [6]. This implies that Sr substituted layered perovskites can be used as potential cathode materials for Solid Oxide Fuel Cells (SOFCs). Based on these results, our group has reported excellent ASRs of composite cathodes of  $\text{SmBaCo}_2\text{O}_{5+\delta}$

(SBCO) [7] and  $\text{SmBa}_{0.5}\text{Sr}_{0.5}\text{Co}_2\text{O}_{5+\delta}$  (SBSCO) [8]. The ASR of SBCO on  $\text{Ce}_{0.9}\text{Gd}_{0.1}\text{O}_{2-\delta}$  (CGO91) is  $0.13 \Omega \text{ cm}^2$  at  $700 \text{ }^\circ\text{C}$ ; the value of a composite cathode (50 wt% of SBCO and 50 wt% of CGO91, SBCO:50) has been observed to be  $0.05 \Omega \text{ cm}^2$  at  $700 \text{ }^\circ\text{C}$ . Advanced electrochemical properties for use in cathode materials for IT-SOFCs have also been observed in the SBSCO oxide system. The lowest ASR value observed in our research was found when a composite cathode of 50 wt% of SBSCO and 50 wt% of CGO91 (SBSCO:50) was used in conjunction with an interlayer of CGO91 applied between the electrode and an 8 mol%  $\text{Y}_2\text{O}_3$  stabilized  $\text{ZrO}_2$  (8YSZ) electrolyte; the obtained values of ASR were as low as  $0.120 \Omega \text{ cm}^2$  at  $600 \text{ }^\circ\text{C}$  and  $0.019 \Omega \text{ cm}^2$  at  $700 \text{ }^\circ\text{C}$  [8]. These results represent a clear improvement compared to results found in the literature of  $0.530 \Omega \text{ cm}^2$  at  $645 \text{ }^\circ\text{C}$  [3] for  $\text{GdBaCo}_2\text{O}_{5+\delta}$  (GBCO) and  $0.150 \Omega \text{ cm}^2$  at  $600 \text{ }^\circ\text{C}$  for  $\text{PrBaCo}_2\text{O}_{5+\delta}$  (PBCO) /  $\text{Ce}_{0.8}\text{Gd}_{0.2}\text{O}_{2-\delta}$  (CGO82) composite cathodes on a CGO82 electrolyte [1]. The new composite cathode, SBSCO:50, shows lower ASR results than those of both conventional cathodes and layered perovskite cathodes for IT-SOFCs [8].

Based on the ASR results for SBSCO:50 [8], a composite cathode comprised of 50 wt% SBSCO and 50 wt% CGO91, was chosen for further tests relevant to cathode materials in metal supported solid oxide fuel cells (MS-SOFCs) because MS-SOFCs

show not only advanced thermal resistance, good mechanical strength and improved sealing efficiency but also a relatively quick start up property when compared to those qualities of general SOFCs [9-14]. However, oxidation of the metal substrate, the Ni-Cr-Fe material and the anode substrate comprised of MS-SOFCs can occur in the high temperature range fabrication condition [15,16], which indicates that all of fabrication processing has to be carried out under hydrogen or inert gas. In the case of the cathode, Co containing perovskite can be decomposed under these gas conditions. Therefore, cathodes have to be prepared using an “in-situ” technique, which means that the coating process was carried out by screen printing and subsequent drying, but without additional heat treatment, in order to prevent the oxidation of MS-SOFC components and the substrate. In summary, the term “in-situ” in this study signifies that the cathodes in the symmetrical half cells were not subject to any sintering process before testing.

Significantly, the electrochemical properties of the in-situ cathode were investigated with respect to the temperature and measuring times because cathodes used for MS-SOFCs cannot be sintered in air at 1000-1200 °C under the single cell preparation processes of MS-SOFCs [17, 18]. The objective of this work is to study the electrochemical properties and the long term performance of the in-situ composite

cathode SBSCO:50 to determine its durability and performance as a cathode for MS-SOFC application.

## **2. Experimental**

### **2.1. Sample preparation**

Samarium oxide ( $\text{Sm}_2\text{O}_3$ ), barium carbonate ( $\text{BaCO}_3$ ), strontium carbonate ( $\text{SrCO}_3$ ), and cobalt oxide ( $\text{Co}_3\text{O}_4$ ) were used for the synthesis of  $\text{SmBa}_{0.5}\text{Sr}_{0.5}\text{Co}_2\text{O}_{5+\delta}$  (SBSCO). For the composite cathode, 50 wt% of SBSCO and 50 wt% of  $\text{Ce}_{0.9}\text{Gd}_{0.1}\text{O}_{2-\delta}$  (CGO91) powders were mixed and suitable inks were made by mixing these powders with an appropriate solvent and binder system. The composite cathode inks were coated onto dense CGO91 pellets sintered at 1400 °C for 4 hours. The final geometry of the sintered CGO91 electrolyte pellets was approximately 21 mm diameter and 2 mm thickness. The thicknesses of the sintered SBSCO:50 and in-situ SBSCO:50 were about 25 and 30  $\mu\text{m}$ , respectively and the final surface area of the symmetric cell was about 1.09  $\text{cm}^2$ .

For all measurements related to the in-situ cathode, the cathode coated on the CGO91 pellet was directly used after drying in an oven, without a subsequent sintering step. Pt-paste and Pt-mesh were used for current collection. Pt mesh, having a surface area of

1.09 cm<sup>2</sup>, was placed on the cathodes and Pt paste was also used between the mesh and each cathode as a current collector.

## **2.2. Electrochemical characterization**

The electrochemical properties of these samples were measured at 650, 700 and 750 °C. In order to evaluate the effect of sintering on the in-situ cathode, an SBSCO:50 cathode was sintered at 1000 °C for 1 hour. The thicknesses of the sintered SBSCO:50 was about 25 μm and the final surface area of the symmetric cell was about 1.09 cm<sup>2</sup>. The measurements of the electrochemical properties and of the area specific resistances (ASRs) of the cathodes were performed at open circuit voltage (OCV) at various temperatures under open air condition using a Solatron 1260 frequency analyzer over a frequency range of 0.01 Hz to 1 MHz and an amplitude of 50 mV.

The ASR was calculated from the difference between the intercepts of the high frequency and low frequency parts and the  $Z'$  axes of the Nyquist plots and the result divided by 2. The ohmic resistances were extracted from the same electrochemical impedance spectroscopy plots using only the intercept of the high frequency parts of the spectra with the  $Z'$  axes.

## **2.3. Microstructural characterization**



The microstructure of the symmetrical half cells was investigated using field emission scanning electron microscopy (FE-SEM, S-4300, Hitachi) combined with energy dispersive spectroscopy (EDS).

### **3. Results and discussion**

#### **3.1. Comparison of electrochemical properties**

Fig. 1 shows the area specific resistance (ASR) results measured at 700 °C; tests were performed under stagnant air in order to study the electrochemical properties and the long-term performance of a composite cathode comprised of 50 wt% of  $\text{SmBa}_{0.5}\text{Sr}_{0.5}\text{Co}_2\text{O}_{5+\delta}$  (SBSCO) and 50 wt% of  $\text{Ce}_{0.9}\text{Gd}_{0.1}\text{O}_{2-\delta}$  (CGO91) (hereafter in this study, this composite cathode is referred to with the abbreviation SBSCO:50) on a dense CGO91 electrolyte. The results for in-situ SBSCO:50 are shown in the same figure using black open circles; this sample was prepared as an in-situ cathode. The other sample, drawn with black closed circles in the figure, was sintered at 1000 °C for 1 hour by following the conventional preparation process before the start of the testing [7, 8]; this was done in order to compare its ASR values to the ASR values of the in-situ cathode.

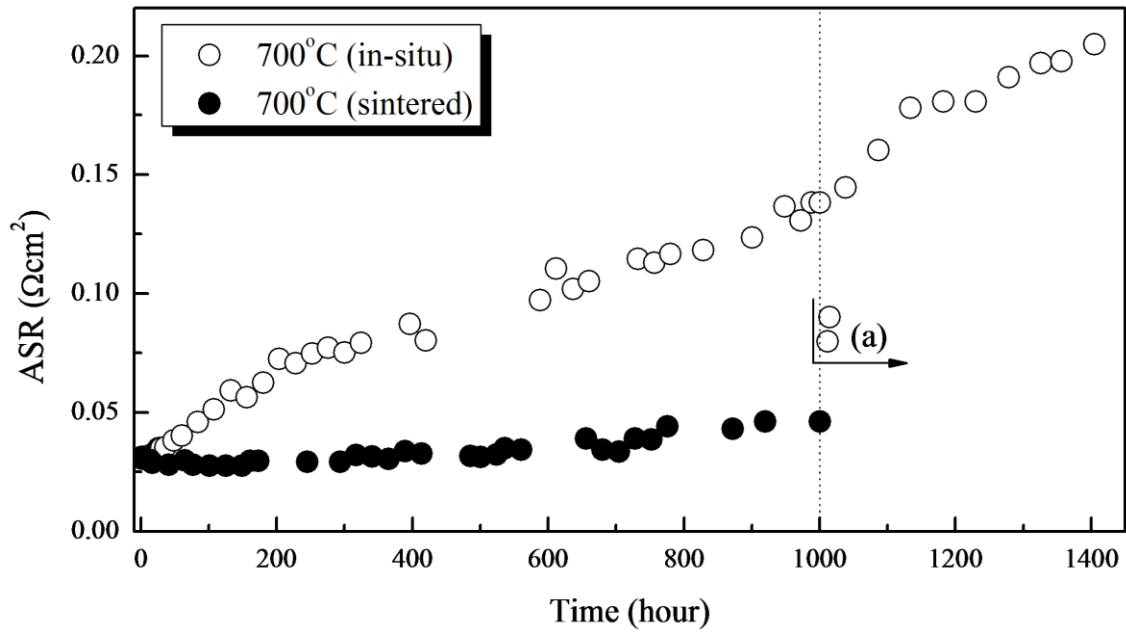


Fig. 1. Area specific resistances (ASRs) of the SBSCO:50 cathode on top of a CGO91 electrolyte with respect to the measuring times. The results, displayed as black open circles, originate from the in-situ SBSCO:50 cathode; the closed circles indicate results coming from a sintered SBSCO:50 cathode. All results were measured at 700 °C.

The initial ASR of the in-situ SBSCO:50 cathode (black open circles) and sintered SBSCO:50 cathode (black closed circles) was observed to be 0.031  $\Omega\text{cm}^2$  at 700 °C, this value increased with measuring time. It is remarkable that the values for the ASR in the in-situ cell and in the conventionally sintered cell are identical at the start of the

experiment, indicating an initially good distribution between SBSCO particles providing rapid oxygen transport kinetics [1-8] and CGO particles providing ionic conductivity and extending the triple phase boundary, in both samples. During the progress of the experiment, however, the in-situ cell shows an increase in ASR, probably because the long term exposure to 700 °C clumps the CGO and the SBSCO particles together without proper sintering effect, thus significantly reducing the length of the triple phase boundary. The conventionally sintered sample does not suffer from this degradation, because the sintering at 1000 °C has provided a permanently good distribution and contact between CGO and SBSCO particles, the microstructure of this sample undergoes very little change during long term exposure to 700 °C.

Significantly, after a measuring time of 200 hours, the ASR in this sample (in-situ SBSCO:50) showed a rapid increase with respect to the measuring time from the initial stage to approximately  $0.075 \Omega \text{ cm}^2$ ; finally, the ASR value increased to  $0.138 \Omega \text{ cm}^2$  after a measuring time of 1000 hours. The ASR behavior of the in-situ SBSCO:50 cathode can be divided into the two parts shown in Fig. 1. Steeply increasing ASRs were observed from the initial stage to 200 hours of measuring time; then, the slope gradually decreased from 200 hours to 1000 hours. In the case of the sintered SBSCO:50 cathode, however, shown as black closed circles, a gentle ASR slope was

observed with an initial ASR of  $0.031 \Omega \text{ cm}^2$  observed at the start of the experiment; the final ASR value measured at  $700 \text{ }^\circ\text{C}$  after 1000 hours was  $0.046 \Omega \text{ cm}^2$ . The difference between the ASR at the initial stage of the measurement of the sintered SBSCO:50 cathode and the ASR value after 1000 hours turned out to be only  $0.015 \Omega \text{ cm}^2$ .

The section in Fig. 1 marked with an (a) indicates the results of another in-situ experiment. After 1000 hours of measurement at  $700 \text{ }^\circ\text{C}$ , the in-situ sample was sintered at  $1000 \text{ }^\circ\text{C}$  for 1 hour and its ASR values were measured for another 404 hours to determine any possible effect of sintering on the already tested in-situ cell. After one hour of sintering at  $1000 \text{ }^\circ\text{C}$ , the ASR of the in-situ sample decreased to  $0.080 \Omega \text{ cm}^2$  (1012 hours). Compared to the final value of  $0.138 \Omega \text{ cm}^2$  of the in-situ sample measured at 1000 hours, the relatively lower ASR value indicates that a micro-connection between the cathode components of CGO91 and SBSCO and the electrolyte developed as a result of the heat-treatment at  $1000 \text{ }^\circ\text{C}$  for 1 hour. However, even though this sample was sintered at  $1000 \text{ }^\circ\text{C}$ , the resulting ASR values quickly increased from  $0.080 \Omega \text{ cm}^2$  (after sintering for 1012 hours) to  $0.200 \Omega \text{ cm}^2$  (1404 hours). This ASR result, which is higher than that of the sample that was sintered before the start of the testing, is directly related to cathode degradation, which is caused by long term measurement and which it was not possible to reverse even when a sintering process

was later applied to the in-situ sample.

The different ASRs of the two specimens can also be related with the differences in the ohmic resistances, which are measured using the intersection of the  $Z'$ -axis and the high frequency arc in the Nyquist plot. To evaluate the influence of the sintering effect, the ohmic resistances of both the SBSCO:50 in-situ cathode and the sintered SBSCO:50 cathode are displayed as a function of time in Fig. 2. The in-situ sample of SBSCO:50 (sample measured for 1000 hours at 700 °C, then sintered at 1000 °C for one hour, then subject to continued testing at 700 °C for another 404 hours), displayed as black open circles in Fig. 2, shows decreasing ohmic resistance values as a function of the measuring time. As discussed previously, there were two types of increased results for the ASRs, divided by the time mark of 200 hours, as can be seen in Fig. 1. The abruptly increasing ASR values shown in Fig. 1, and the decreasing ohmic results shown in Fig. 2 for the in-situ sample, occur in the same time interval between the start of the test and the measuring time of 200 hours. This indicates that within the first 200 hours of elevated temperature (700 °C) both the microstructure at the interface between the cathode and the electrolyte and the internal microstructure of the cathode were subject to major changes. The overall electrochemical performance during this phase was dominated by the reduction of the ohmic resistance caused by contact improvement at

the interface between electrolyte and cathode. In the measurement period between 200 and 1000 hours, the ohmic resistances of the in-situ sample did not change with the measuring time (as shown in Fig. 2); on the other hand, the ASRs of the in-situ cathode increased with respect to the measuring time (as shown in Fig. 1). This indicates that, from the first stage of measurement to the point of 200 hours of measurement, the main influence on the changes in the electrochemical performance during sintering was the microstructural improvement of the interface between the CGO91 electrolyte and SBSCO:50. In the case of the sintered sample, shown as black closed circles in Fig. 2, the ohmic resistances decreased in the initial stage. It is difficult to explain exactly the reasons for the decrease in the ohmic resistance in the sintered cell within the initial 100 hours of testing. The decrease might be related to a stabilization process of the sintered SBSCO:50 cathode at the start of the measurement. Significantly, the values measured for the ohmic resistance of the sintered cell at 700 °C stay almost constant after the initial 100 hours of measurement. From 1000 hours of measuring time onward, the ohmic resistances of the in-situ cathode are marked with an (a) in Fig. 2. After the heat-treatment of the in-situ sample, the ohmic resistance decreased to  $3.032 \Omega \text{ cm}^2$  after 1012 hours total testing time; this value remained almost the same after that time for another 400 hours of testing, indicating that the sintering process was completed after

the heat-treatment.

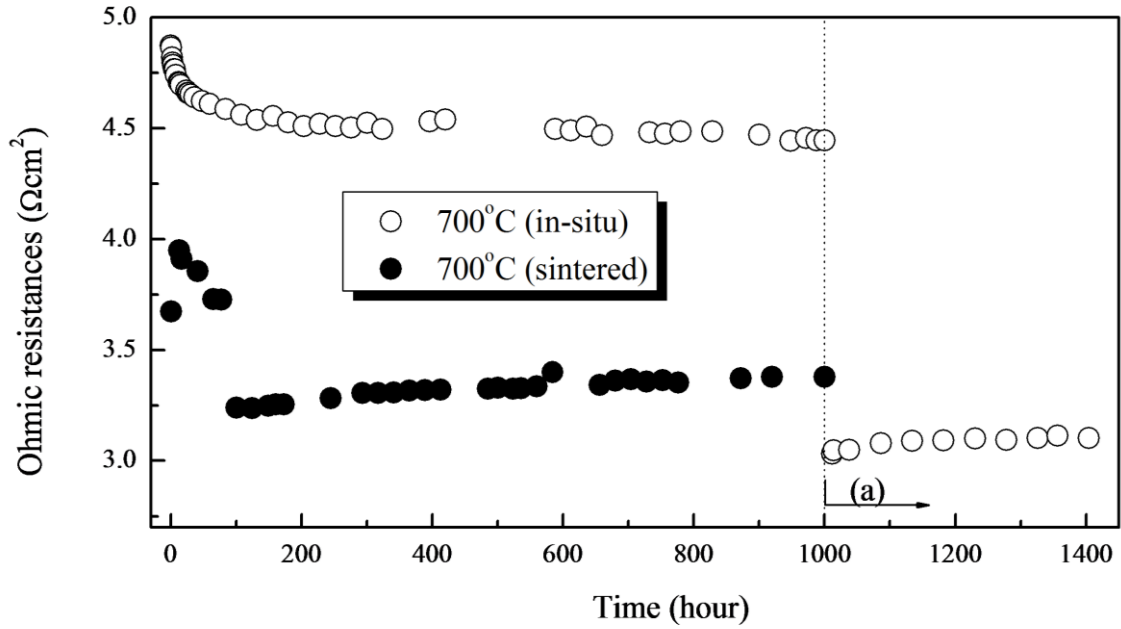
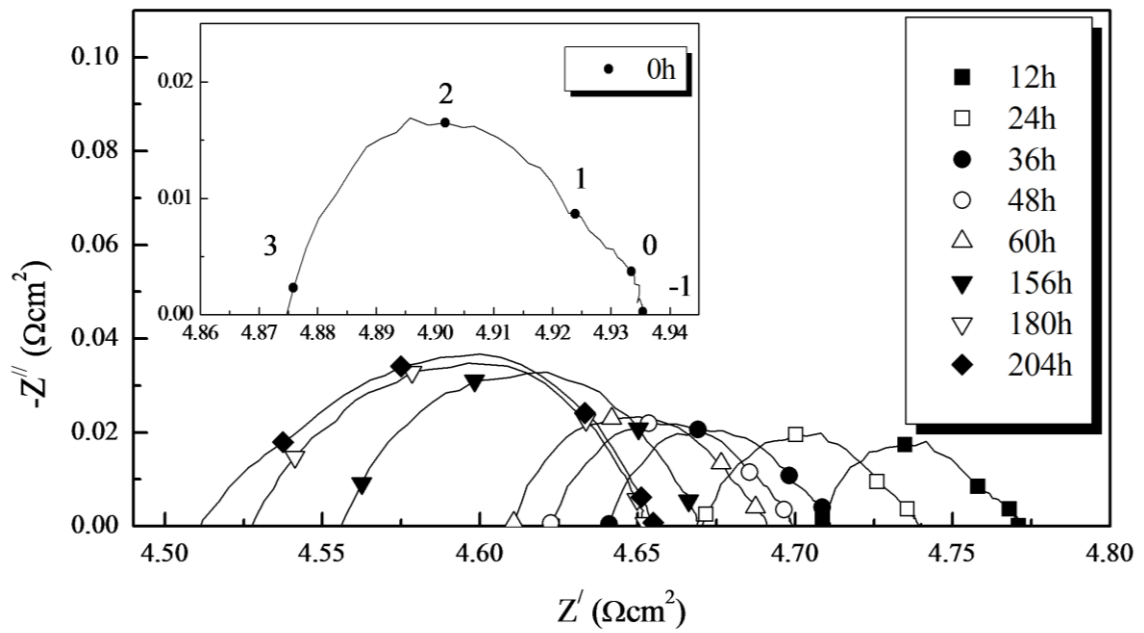


Fig. 2. Ohmic resistances of the in-situ sample and of the sintered sample measured at 700 °C.

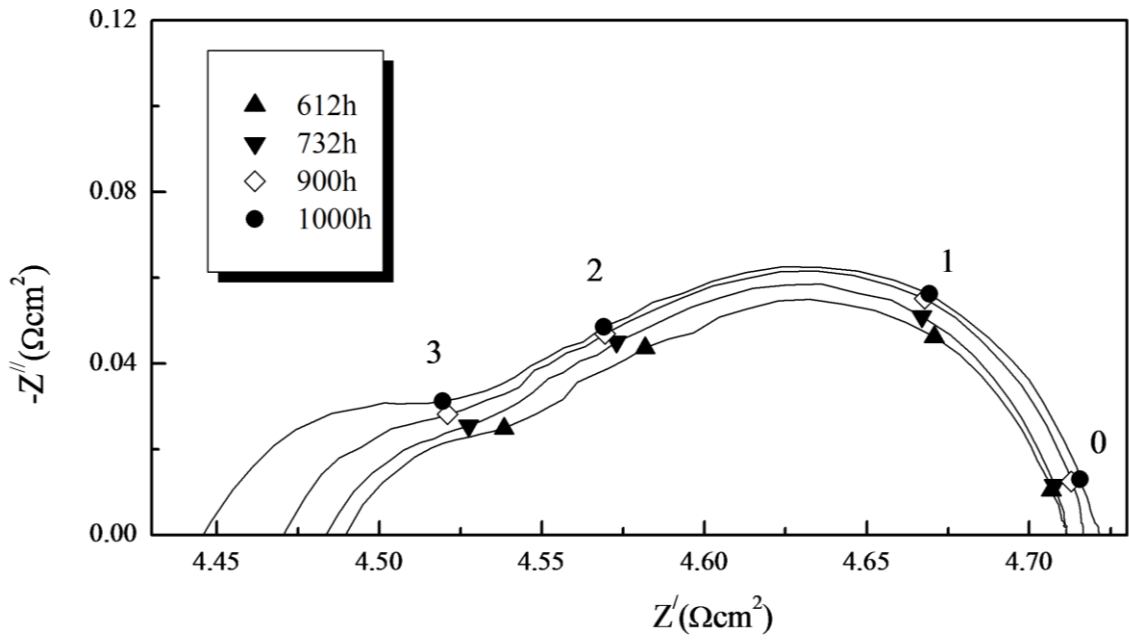
This implies that the major part of the sintering effect [on the overall electrochemical performance of the](#) in-situ cathode is not the result of changes at the cathode surface or the inside of the cathode but is rather dominated by changes at the interface between the cathode and the electrolyte after heat treatment. [Unsurprisingly the ohmic resistance is generally reduced by sintering at 1000 °C, because of the huge improvement of contact](#)

at the interface between electrolyte and cathode. The described experiment proves that this positive effect on the ohmic resistance is achieved, no matter if the sintering step is carried out before the start of the experiment or after 1000 hours of operation at 700 °C.

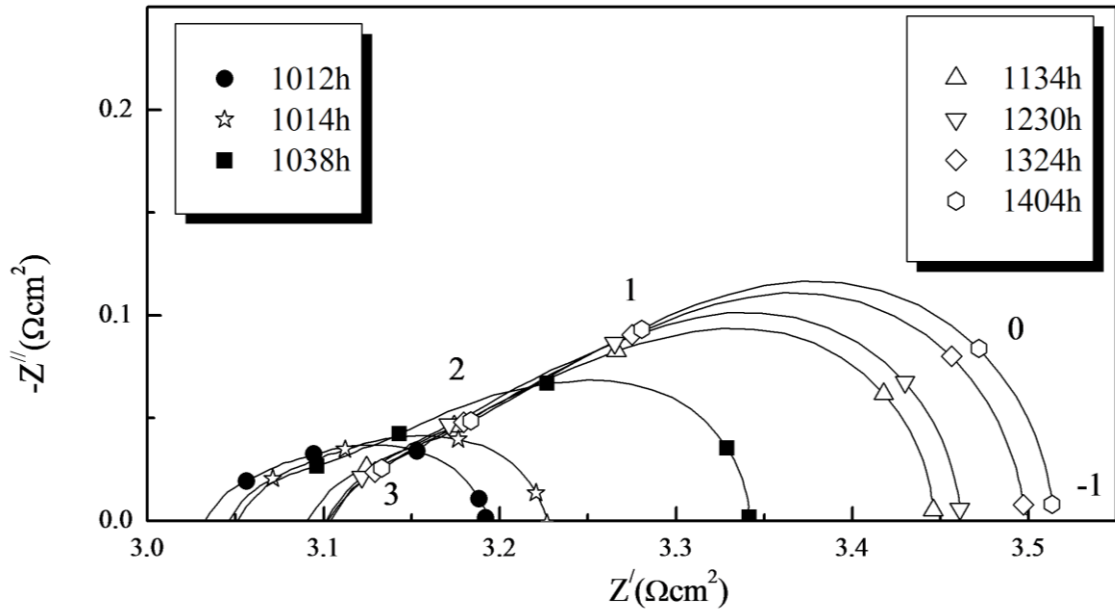


(a)





(b)



(c)

Fig. 3. Impedance plots for the in-situ SBSCO:50 cathode on a CGO91 electrolyte measured at 700 °C. (a) and (b) show the impedance properties from the initial stage of measurement up to 1000 hours. (c) displays the impedance results for the in-situ cathode after sintering at 1000 °C for 1 hour.

To further investigate the relation of the ASRs and the ohmic resistances, Fig. 3 displays impedance plots of the in-situ and sintered SBSCO:50 cathodes on a CGO91 electrolyte at different measuring times. The lines in these figures indicate experimental results; some of the points on these lines are substituted with symbols combined with superscript numbers; these denote the logarithm of the frequency at which these data points were received. A symbol with a superscript 2 thus signifies that the impedance data related leading to this point of the plot were received at a frequency of 100 Hz. Fig. 3. (a) shows the impedance Nyquist plots, which are comprised of low frequency and high frequency arcs taken at 12 hour intervals from the initial stage until 60 hours of measurement time, and at longer intervals up to 180 hours of measurement time. While the shapes of the arcs in the plots taken at different measurement times are similar, their sizes increase, with both high frequency and low frequency arcs increasing in size up to

60 hours; from then on, however, up to 180 hours, only the high frequency part of the plots increase. The ohmic resistance of the in-situ SBSCO:50 cathode decreased as a function of the measuring time due to the cathode's increasingly strong adherence to the CGO91 electrolyte, while the ASRs increased as shown in Fig. 3. (a). The arc measured after 204 hours showed different behavior when compared to the results for the sample after 180 hours of measuring time. The previously described testing time led to rapid increases in the ASR results; decreases of the ohmic resistance shown in Fig. 1 and Fig. 2 can also be found in Fig. 3. (a), indicating that additional interface adhesion and cathode coarsening occur simultaneously within this measurement period.

When comparing the impedance results up to 204 hours, as shown in Fig. 3. (a), and those results up to 1000 hours of measuring time, as shown in Fig. 3. (b), the largest separation between the impedance plots of different measuring times was observed in the vicinity of  $10^3$  Hz; the high frequency arc becomes more and more dominant with increasing measuring time. This is not only caused by oxygen ion conduction/migration, which is related to the electrolyte, but also to the sintering processes in the composite cathode and between the cathode and the electrolyte; obviously, both the interfaces of the cathode/electrolyte and the cathode/cathode are affected [19, 20]. Additionally, the size of the impedance arcs measured at the low frequency ranges increased with respect

to the measuring times and the ohmic resistance measured at high frequency ranges decreased because the interface (cathode/electrolyte) and the bulk of the cathode (cathode/cathode) were sintered together. However, in this case, sintering phenomena mainly occurred at the interface of the electrode/electrolyte rather than at the interface of the electrode/electrode.

Fig. 3. (c) displays impedance plots of the in-situ cathode after it was sintered at 1000 °C for 1 hour after reaching 1000 hours of measuring time. The 1000 °C sintering temperature with the in-situ SBSCO:50 cathode resulted in an ohmic resistance of 3.032  $\Omega \text{ cm}^2$  and an ASR of 0.080  $\Omega \text{ cm}^2$ ; both of these values represent decreases compared to the values (an ohmic resistance of 4.445  $\Omega \text{ cm}^2$  and an ASR of 0.138  $\Omega \text{ cm}^2$ ) of the unsintered in-situ cathode upon reaching 1000 hours of measuring time, as shown in Fig. 3. (b). In other words, the post sintering process applied to the in-situ cathode did momentarily decrease the total ASR, but these ASR results did not maintain a constantly low value after the continuation of the measurement. In more detail, with increasing measurement time after heat treatment, the ohmic resistance did not change and remained in the vicinity of 3.100  $\Omega \text{ cm}^2$ . However, the ASR values increased, especially due to the increase of the low frequency impedance arcs measured at frequencies such as  $10^0$  and  $10^{-1}$  Hz. After heat treatment at 1000 °C for 1 hour, the low frequency arc

became more dominant with respect to the measurement time because of gas diffusion problems caused by the changed microstructure in the composite cathode.

### **3.2. Relationships between microstructure and electrochemical properties**

Fig. 4 shows SEM images of the SBSCO:50 cathodes with respect to their different fabrication procedures. Figs. 4. (a) and (c) show cross views of the in-situ SBSCO:50 and Figs. 4. (b) and (d) show cross views of an SBSCO:50 sample sintered at 1000 °C for 1 hour before the start of the testing. Both cathodes are on top of the dense CGO91 electrolyte, as can be seen in Figs. 4. (a) and (b). Additional figures show top views of the cathodes: Figs. 4. (e) and (g) of the in-situ cathode and Figs. 4. (f) and (h) of the sintered cathode. From the cross views and top views shown in (d) and (h), the particle size of SBSCO can be estimated to be around 1~2  $\mu\text{m}$ ; the surface is decorated with much smaller CGO91 particles.

According to the SEM images of the two samples shown in Fig. 4, no clear microstructural distinction in the interfaces of SBSCO:50 and CGO91 can be directly observed in Figs. 4. (a) and (b). However, the agglomeration of small particles identified as CGO91 is shown in Fig. 4. (d). Especially, Fig. 4. (d) shows evidence of a sintering effect, because small sized CGO91 particles with diameters of around 100 nm can be seen to be agglomerated and relatively larger sized particles of SBSCO are closely

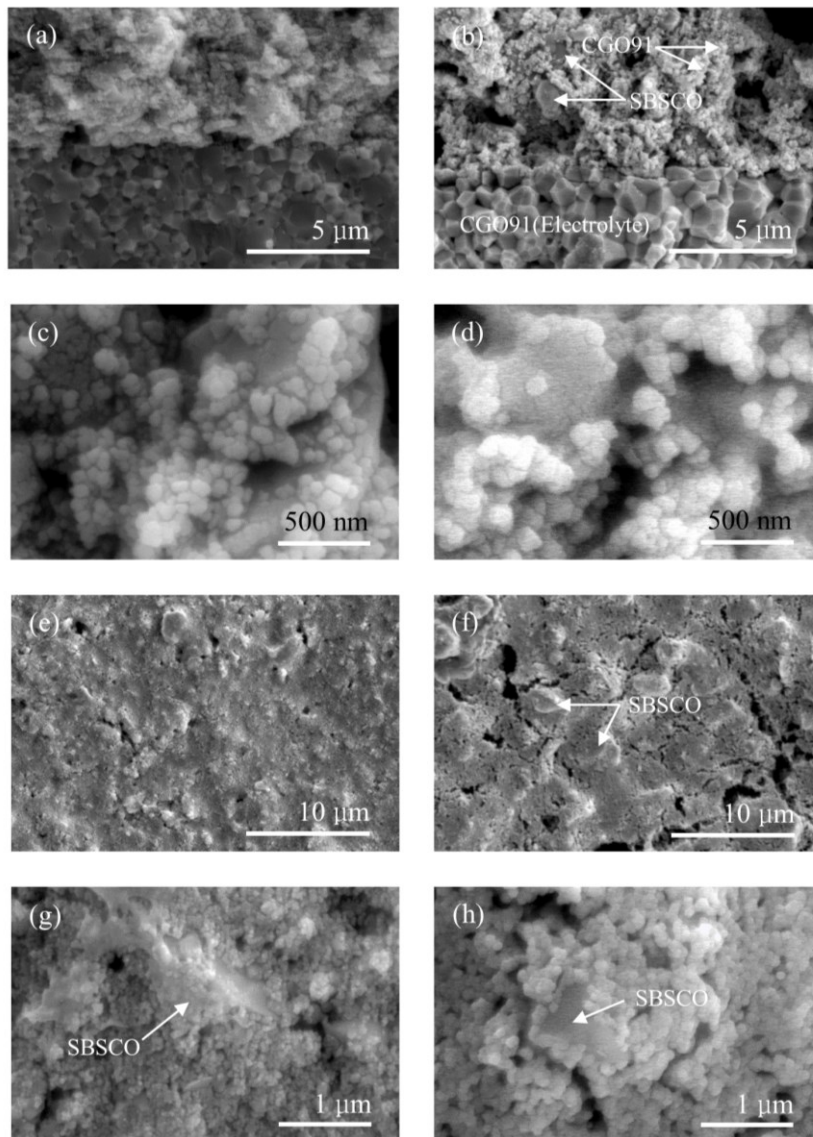


Fig. 4. SEM images of the in-situ sample and of the sintered cathode. (a), (b), (c) and (d) are cross view images of the in-situ sample and of the sintered cathode. (e), (f), (g) and (h) are top view results. The sintered sample in this paper was sintered at 1000 °C for 1 hour. SBSCO was found to form 1~2 μm sized particles; the small sized particles consist of CGO91.

connected with the CGO91 particles.

The top view images in Fig. 4 show a clear difference between the in-situ and the sintered SBSCO:50 cathodes. The top view of the in-situ cathode shown in Fig. 4. (e) shows the mixture state itself. Significantly, the different microstructures in Figs. 4. (g) and (h) result in the ASR differences between the two samples described above. For example, the increased ASR of the in-situ cathode is caused by the CGO91 and SBSCO powders clumping together without any sintering taking place; on the other hand, the ASR of the sintered SBSCO:50 cathode is shown to be relatively stable over the long testing period, as can be seen in Fig. 1; this stability was not only caused by a compact connection between the SBSCO particles, but was also generated by the good connection of these particles with CGO91. In other words, the different ASR behaviors of the two samples are directly caused by the microstructure. For example, micro networking between the SBSCO:50 composite cathode and the CGO91 electrolyte, or between the different components of the composite cathode, was not fully developed in the in-situ SBSCO:50 sample resulting in a poor microstructure on the surface of the electrolyte.

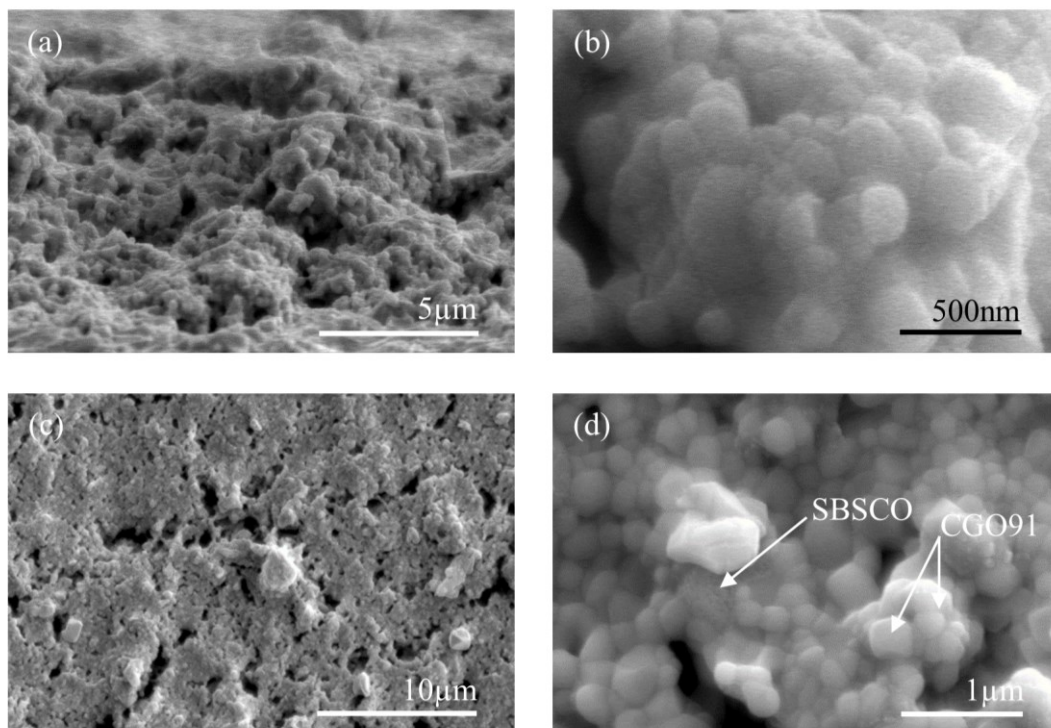


Fig. 5. SEM images of the in-situ SBSCO:50 cathode after completion of sintering and of the long-term test. (a) and (b) are cross views and (c) and (d) are top views of the cathode. Significantly, this sample was sintered at 1000 °C for 1 hour after 1000 hours of measuring time.

As shown in Fig. 3. (c), the low frequency arc becomes dominant with respect to the measurement time because of gas diffusion problems caused by the microstructure in the composite cathode, which changes after heat treatment at 1000 °C for 1 hour. The relationships between the low frequency arc behavior and the microstructure are linked;



these microstructure changes are visualized in the SEM images shown in Fig. 5. Figs. 5 (a) and (b) show cross views of the in-situ sintered SBSCO cathode after completion of the experiment. Figs. 5. (c) and (d) are top views of this sample. As previously shown in Fig. 3. (c), the increased low frequency arc after the heat treatment is caused by cathode densification. The reason for this densification, as shown in Fig. 5, are an increased connection of the CGO91 particles and a surface densification caused by the heat-treatment and the long-term experiment. Significantly, compared to the particle sizes shown in Figs. 4. (e) and (g), a coarsening of discontinuous particles was observed in the in-situ sintered cathode.

From these results, various electrochemical properties of the in-situ composite SBSCO:50 cathode can be summarized. The ASR results for the in-situ and the sintered cathodes showed almost the same values at the initial stage of the measurement. However, the ASR values of the sintered SBSCO:50 cathode showed a constant value as a function of measuring time, while the ASR of the in-situ cathode increased up to 1000 hours. From the initial stage to the point of 200 hours of measuring time, decreasing ohmic resistance was observed as well as increased total ASR in the in-situ cathode system. An additional frequency arc at relatively high frequency was also observed due to oxygen ion conduction and migration related to adhesion between the cathode and the

electrolyte. The heat-treatment of the in-situ cathode at 1000 °C may have temporarily reduced the ASR; however, the overall ASR values quickly returned to the pre-sintering values and, subsequently, increased in spite of the sintering process. In contrast, the shape and size of the impedance arcs of SBSCO:50 sintered at 1000 °C before the start of the measurement did not change during the 1000 hours of measurement, though the ohmic resistance did increase, as shown in Fig. 6.

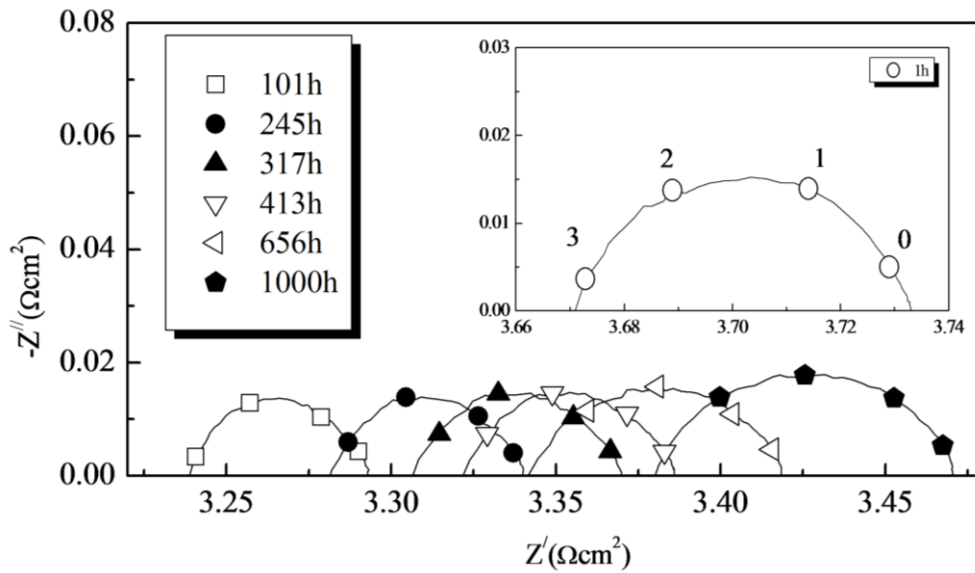


Fig. 6. Impedance plots of a sample sintered at 1000 °C for 1 hour measured at various measuring times. The in-set numbers denote the logarithm of the measuring frequency.

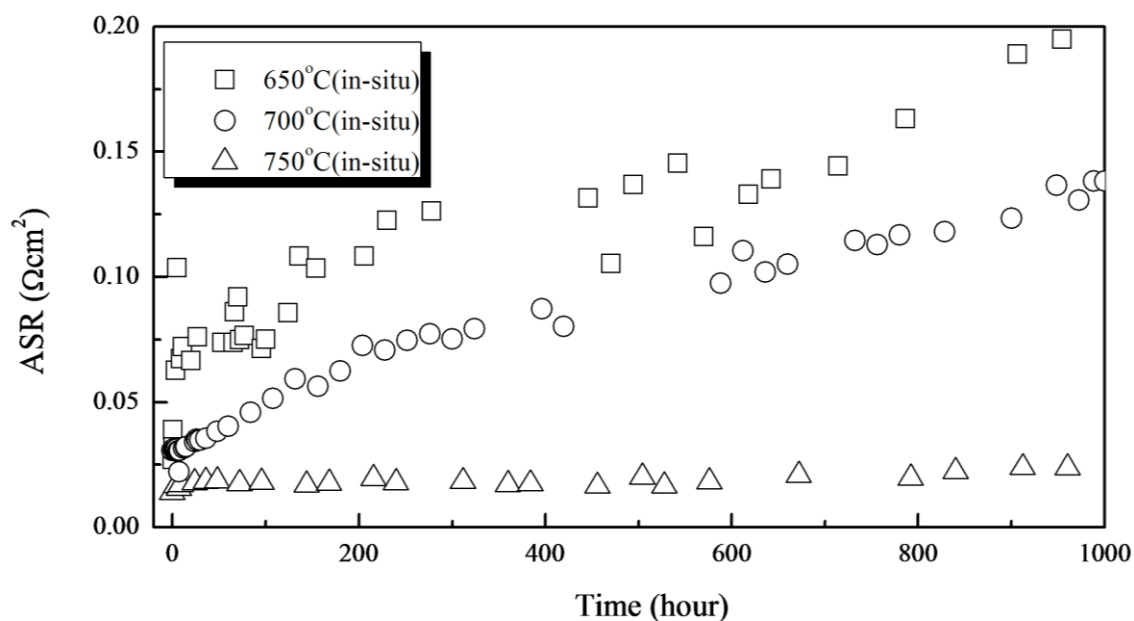


Fig. 7. ASRs of the in-situ SBSCO cathode measured at various temperatures (650, 700 and 750 °C) for 1000 hours.

### 3.3. Electrochemical properties of in-situ SBSCO:50

Experiments were also carried out to investigate the effects of sintering and long term measurements with various measuring temperatures such as 650 and 750 °C on the electrochemical properties, with results shown in Figs. 7, 8, and 9. Fig. 7 shows the ASR results for the in-situ cathode measured at 650 °C, 700 °C, and 750 °C; these results were used to compare the ASR behavior and to decide on the optimum sintering temperature for the in-situ SBSCO:50 cathode. From the ASR results shown in Fig. 7,

the ASR measured at 650 °C can be seen to increase as a function of the measuring time; this is also true for the ASR measured at 700 °C, although some fluctuation occurred during the measurement. The increase of the ASR of the in-situ cathode measured at 650 °C very much resembles the behavior at 700 °C, with a rapid increase in the first 200 hours of measurement from an initial value of 0.027  $\Omega \text{ cm}^2$  to a value of 0.108  $\Omega \text{ cm}^2$ , as shown in Figs. 1 and 7. This indicates that the sintering process of the in-situ cathode measured at 650 °C can be said to follow the same mechanism as that in the cathode measured at 700 °C. From 200 to 750 hours of measuring time, the in-situ cathode measured at 650 °C maintained a constant ASR value and, significantly, the ASR increased from 750 hours onwards. In contrast to the measurements at 650 °C and 700 °C, the results for the in-situ cathode measured at 750 °C showed an almost constant ASR, with values of 0.014, 0.020 and 0.024  $\Omega \text{ cm}^2$  at 0, 500, and 1000 hours of measurement time. This indicates that the optimum sintering temperature for the in-situ cathode has to be over 750 °C.

Fig. 8 shows the ohmic resistance results measured at 650 °C, 700 °C and 750 °C. The initial ohmic resistance measured at 650 °C is lower than the value measured at 700 °C; this discrepancy is mainly due to the difference in the CGO91 electrolyte thickness. The ohmic resistance measured at 650 °C for the in-situ sample changed slightly from the

initial state to the point of 120 hours of measuring time; then, this value suddenly increased from  $4.399 \Omega \text{ cm}^2$  to  $5.000 \Omega \text{ cm}^2$ . After that, the values stayed almost constant, ending at  $5.194 \Omega \text{ cm}^2$  after 954 hours. In the case of the results measured at  $750^\circ\text{C}$ , the ohmic resistance values seem to stay steady at a low level ( $2.077 \Omega \text{ cm}^2$  at the initial state and  $2.034 \Omega \text{ cm}^2$  after 1000 hours), with only a  $0.043 \Omega \text{ cm}^2$  difference for measurements 1000 hours apart.

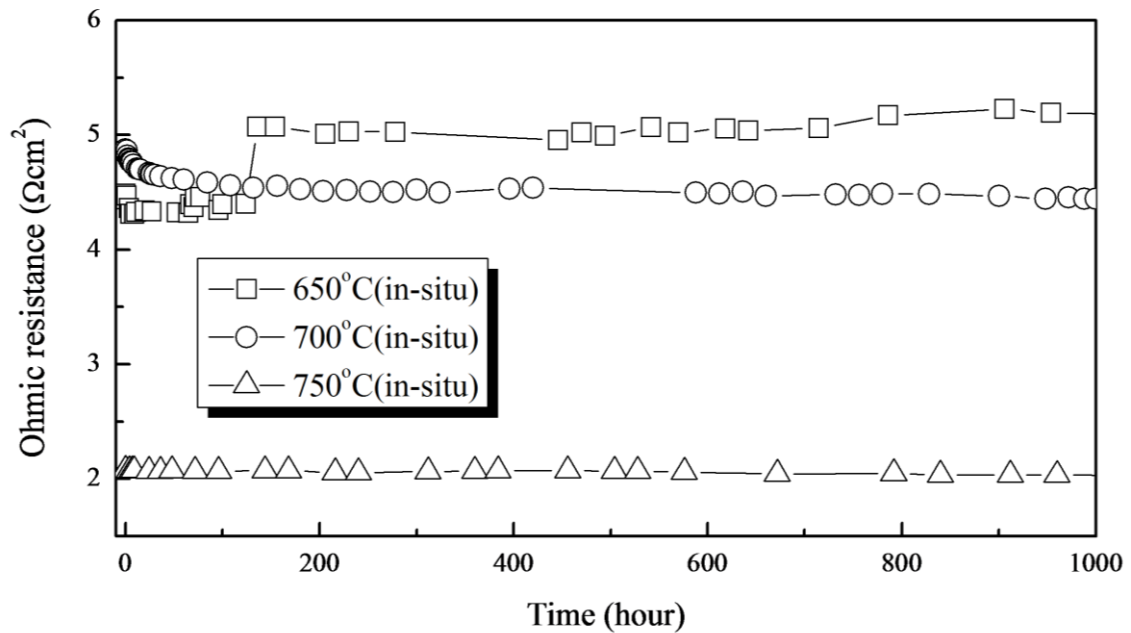


Fig. 8. Ohmic resistances of the in-situ SBSCO:50 cathode sample measured at 650, 700 and  $750^\circ\text{C}$  for 1000 hours. These results were extracted from the intercept of the high frequency part of the spectra with the  $Z'$  axes of the Nyquist plots.

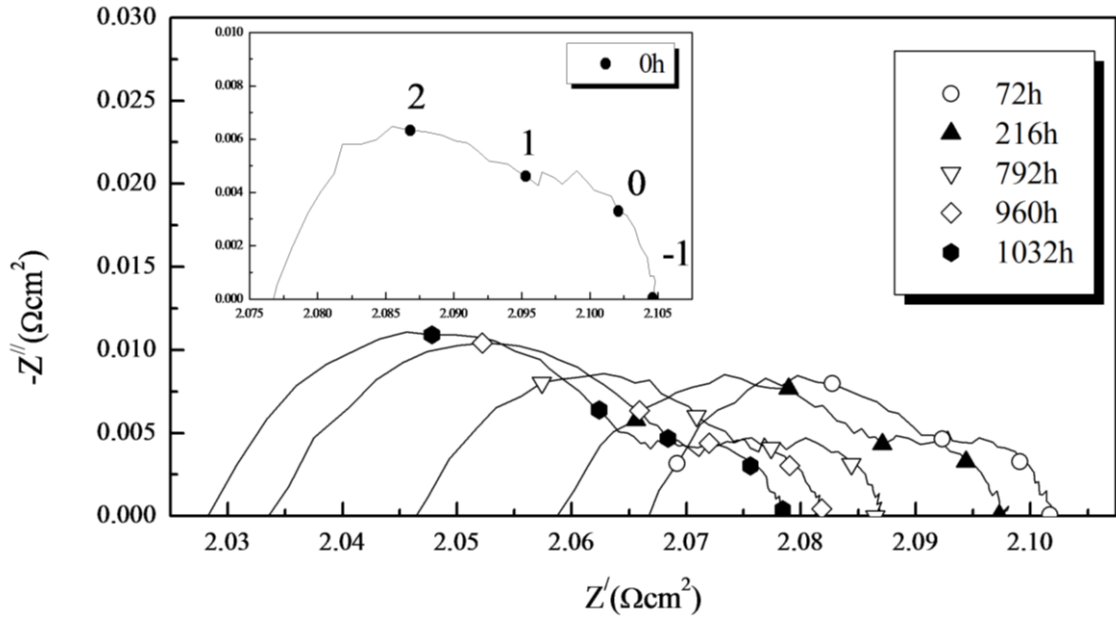


Fig. 9. Impedance plots measured for the in-situ SBSCO:50 cathode at 750 °C. The inset numbers denote the logarithm of the measuring frequency.

Fig. 9 shows the impedance arcs obtained from the in-situ SBSCO:50 cathode measured at 750 °C. The results show that the ASRs caused by electrode polarization resistance increased as a function of time, while the ohmic resistance decreased. However, all of the impedance arcs show similar arc shapes, with the high frequency arcs dominating the total impedance at the initial stage and over the whole measurement period. This implies that in the cathode measured at 750 °C the sintering process was not only effective at the interface between the cathode and the electrolyte but also inside the cathode, between the bulk and the surface.

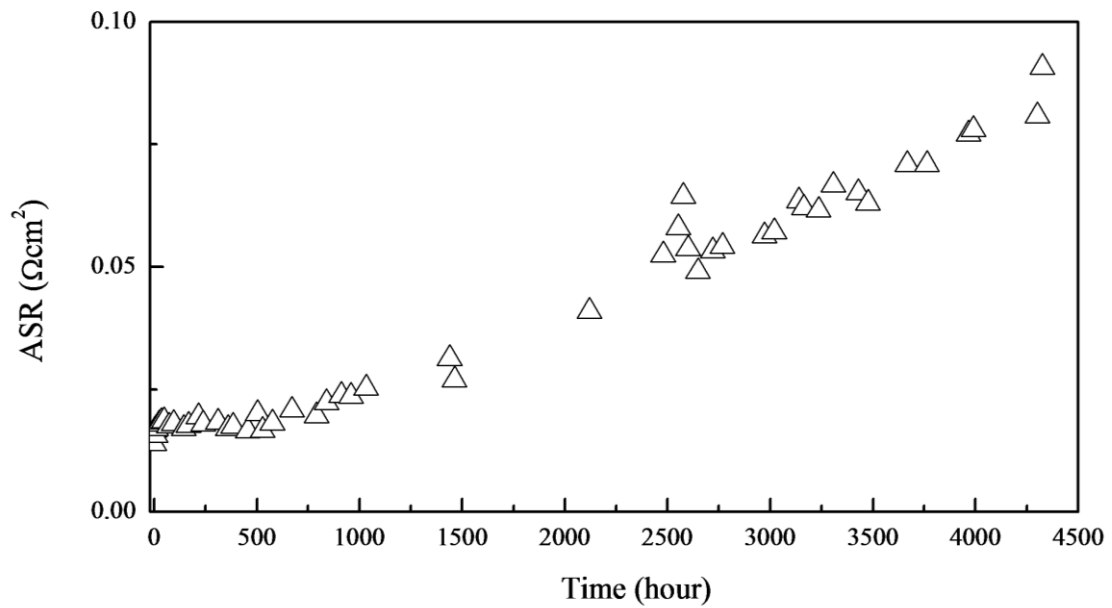


Fig. 10. Long term performance of the in-situ SBSCO:50 cathode extending the measuring time to 4300 hours at 750 °C.

### 3.4. Long term performance of in-situ SBSCO:50

Finally, Fig. 10 shows the long term performance of the in-situ SBSCO:50 cathode measured at 750 °C and displayed as impedance diagrams achieved in long-term tests.

As shown in Fig. 7, the ASRs of the composite cathode remain almost constant over the first 1000 hours when measuring is performed at 750 °C. When measurements were taken for periods longer than 1000 hours at 750 °C, the diagram shows an

approximately linear increase of the total ASR. There is an obvious degradation of the performance in this cell with increasing measuring time; however, the deviation between the initial value ( $0.014 \Omega \text{ cm}^2$ ) and the final value measured at 4300 hours ( $0.091 \Omega \text{ cm}^2$ ) is only  $0.077 \Omega \text{ cm}^2$ .

#### 4. Conclusions

In this research, the electrochemical properties and long-term performance of an in-situ composite cathode (SBSCO:50) were investigated for MS-SOFC applications.

Prior to the impedance experiment, the sintered SBSCO:50 cathode showed an ASR of  $0.031 \Omega \text{ cm}^2$  and the increase of the ASR after 1000 hours of measurement at  $700 \text{ }^\circ\text{C}$  was only  $0.015 \Omega \text{ cm}^2$ . Additionally, the ohmic resistances did not change during long-time operation. The ASR of the in-situ composite cathodes increased with respect to the operating time when measured at  $650$  and  $700 \text{ }^\circ\text{C}$ . The ohmic resistances of the in-situ samples decreased at the initial stage, reaching a constant level after 200 hours of measuring time, indicating that within these first 200 hours the microstructure of the cathodes in these in-situ systems was improved. The extent of this improvement is much smaller compared to the improvement observed in the sample operated at  $750 \text{ }^\circ\text{C}$ , indicating the fact that  $700 \text{ }^\circ\text{C}$  are insufficient for reaching an optimized interface microstructure. In contrast to the ASRs measured at lower temperatures, the ASRs



measured for the in-situ cathode at 750 °C displayed stable results for the first 1000 hours. This indicates that the optimum sintering temperature for the in-situ cathode in MS-SOFC applications is over 750 °C.

Most usefully, the operating temperature required for the operation of a MS-SOFC application using the in-situ SBSCO:50 cathode has to be higher than 700 °C. Future work will include further studies about the influence of high temperature on microstructure and on the long-term durability including long term measurements at 800 °C. The comparison of these results with experiments presented in this paper will help to investigate an optimum temperature for the operation of MS-SOFCs with in-situ cathodes.

### **Acknowledgments**

The authors are grateful for the support of the Basic Science Research Program, part of the National Research Foundation of Korea (NRF), funded by the Ministry of Science, ICT & Future Planning (No. 2014R1A1A1004163).

## References

- [1] Kim G, Wang S, Jacobson AJ, Reimus , Brodersen P, Mims CA. Rapid oxygen ion diffusion and surface exchange kinetics in  $\text{PrBaCo}_2\text{O}_{5+x}$  with a perovskite related structure and ordered A cations. *J Mater Chem* 2007;17:2500-05.
- [2] Taskin AA, Lavrov AN, Ando Y. Achieving fast oxygen diffusion in perovskites by cation ordering. *Appl Phys Lett* 2005;86:091910(1)-091910(3).
- [3] Chang A, Skinner SJ, Kilner JA. Electrical properties of  $\text{GdBaCo}_2\text{O}_{5+x}$  for ITSOFC applications. *Solid State Ionics* 2006;117:2009-11.
- [4] Tarancón A, Skinner SJ, Chater RJ, Hernández-Ramírez F, Kilner JA. Layered perovskites as promising cathodes for intermediate temperature solid oxide fuel cells. *J Mater Chem* 2007;17:3157-81.
- [5] Maignan A, Martin C, Pelloquin D, Nguyen N, Raveau B. Structural and magnetic studies of ordered oxygen-deficient perovskites  $\text{LnBaCo}_2\text{O}_{5+6}$ , closely related to the “112” structure. *J Solid State Chem* 1999;142:247-60.
- [6] Zhou WZ, Lin CT, Liang WY. Synthesis and structural studies of the perovskite-related compound  $\text{YBaCo}_2\text{O}_{5+x}$ . *Adv Mater* 1993;5:735-38.
- [7] Kim JH, Kim Y, Connor PA, Irvine JTS, Bae J, Zhou W. Structural, thermal and electrochemical properties of layered perovskite  $\text{SmBaCo}_2\text{O}_{5+d}$ , a potential cathode

- material for intermediate-temperature solid oxide fuel cells. *J Pow Sour* 2009;194:704-711.
- [8] Kim JH, Cassidy M, Irvine JTS, Bae J. Advanced electrochemical properties of  $\text{LnBa}_{0.5}\text{Sr}_{0.5}\text{Co}_2\text{O}_{5+\delta}$  (Ln = Pr, Sm, and Gd) as cathode materials for IT-SOFC. *J Electrochem Soc* 2009;156(6):B682-89.
- [9] Tucker MC, Lau GY, Jacobson CP, DeJonghe LC, Visco SJ, Performance of metal-supported SOFCs with infiltrated electrodes. *J Pow Sour* 2007;171:477-82.
- [10] Hui S, Yang D, Wang Z, Yick S, Decès-Petit C, Qu W, Tuck A, Maric R, Ghosh D, Metal-supported solid oxide fuel cell operated at 400-600 °C. *J Pow Sour* 2007;167:336-39.
- [11] Xie YS, Neagu R, Hsu CS, Zhang X, Decès-Petit C, Spray pyrolysis deposition of electrolyte and anode for metal-supported solid oxide fuel cell. *J. Electrochem Soc* 2008;155: B407-B410.
- [12] Waldbillig D, Kesler O, Characterization of metal-supported axial injection plasma sprayed solid oxide fuel cells with aqueous suspension plasma sprayed electrolyte layers. *J Pow Sour* 2009;191:320-29.
- [13] Hwang C, Tsai CH, Lo CH, Sun CH, Plasma sprayed metal supported YSZ/Ni-LSGM-LSCF ITSOFC with nanostructured anode. *J Pow Sour* 2008;180:132-42.
- [14] Zhao Y, Xia C, Jia L, Wang Z, Li H, Yu J, Li Y, Recent progress on solid oxide fuel cell: Lowering temperature and utilizing non-hydrogen fuels. *Int J Hydrogen Energy* 2013;38:16498-517.

- [15] Kim YM, Kim-Lohsoontorn P, Bae J, Effect of unsintered gadolinium-doped ceria buffer layer on performance of metal-supported solid oxide fuel cells using unsintered barium strontium cobalt ferrite cathode. *J Pow Sour* 2010;195:6420-27.
- [16] Choi JJ, Oh SH, Noh HS, Kim HR, Son JW, Park DS, Choi JH, Ryu J, Hahn BD, W. H. Yoon, H. W. Lee, Low temperature fabrication of nano-structured porous LSM-YSZ composite cathode film by aerosol deposition. *J Alloys Comp* 2011;509:2627-30.
- [17] Baek SW, Jeong J, Kim YM, Kim JH, Shin S, Bae J. Metal-supported solid oxide fuel cells with barium-containing in-situ cathodes. *Solid State Ionics* 2011;192:387-93.
- [18] Nielsen J, Hjalmarsson P, Hansen MH, Blennow P. Effect of low temperature in-situ sintering on the impedance and the performance of intermediate temperature solid oxide fuel cell cathodes. *J Power Sour* 2014;245:418-28.
- [19] Adler SB. Factors governing oxygen reduction in solid oxide fuel cell cathodes. *Chem Rev* 2004;104:4791-843.
- [20] S.B. Adler, *Solid State Ion.* 111 (1998) 125- 134. Adler SB. Mechanism and kinetics of oxygen reduction on porous  $\text{La}_{1-x}\text{Sr}_x\text{CoO}_{3-\delta}$  electrodes. *Solid State Ionics* 1998;111:125-134.

## Figure Captions

Fig. 1. Area specific resistances (ASRs) of the SBSCO:50 cathode on top of a CGO91 electrolyte with respect to the measuring times. The results, displayed as black open circles, originate from the in-situ SBSCO:50 cathode; the closed circles indicate results coming from a sintered SBSCO:50 cathode. All results were measured at 700 °C.

Fig. 2. Ohmic resistances of the in-situ sample and of the sintered sample measured at 700 °C.

Fig. 3. Impedance plots for the in-situ SBSCO:50 cathode on a CGO91 electrolyte measured at 700 °C. (a) and (b) show the impedance properties from the initial stage of measurement up to 1000 hours. (c) displays the impedance results for the in-situ cathode after sintering at 1000 °C for 1 hour.

Fig. 4. SEM images of the in-situ sample and of the sintered cathode. (a), (b), (c) and (d) are cross view images of the in-situ sample and of the sintered cathode. (e), (f), (g) and (h) are top view results. The sintered sample in this paper was sintered at 1000 °C for 1 hour. SBSCO was found to form 1~2  $\mu\text{m}$  sized particles; the small sized particles consist of CGO91.

Fig. 5. SEM images of the in-situ SBSCO:50 cathode after completion of sintering and

of the long-term test. (a) and (b) are cross views and (c) and (d) are top views of the cathode. Significantly, this sample was sintered at 1000 °C for 1 hour after 1000 hours of measuring time.

Fig. 6. Impedance plots of a sample sintered at 1000 °C for 1 hour measured at various measuring times. The in-set numbers denote the logarithm of the measuring frequency.

Fig. 7. ASRs of the in-situ SBSCO cathode measured at various temperatures (650, 700 and 750 °C) for 1000 hours.

Fig. 8. Ohmic resistances of the in-situ SBSCO:50 cathode sample measured at 650, 700 and 750 °C for 1000 hours. These results were extracted from the intercept of the high frequency part of the spectra with the  $Z'$  axes of the Nyquist plots.

Fig. 9. Impedance plots measured for the in-situ SBSCO:50 cathode at 750 °C. The in-set numbers denote the logarithm of the measuring frequency.

Fig. 10. Long term performance of the in-situ SBSCO:50 cathode extending the measuring time to 4300 hours at 750 °C.

## Figures

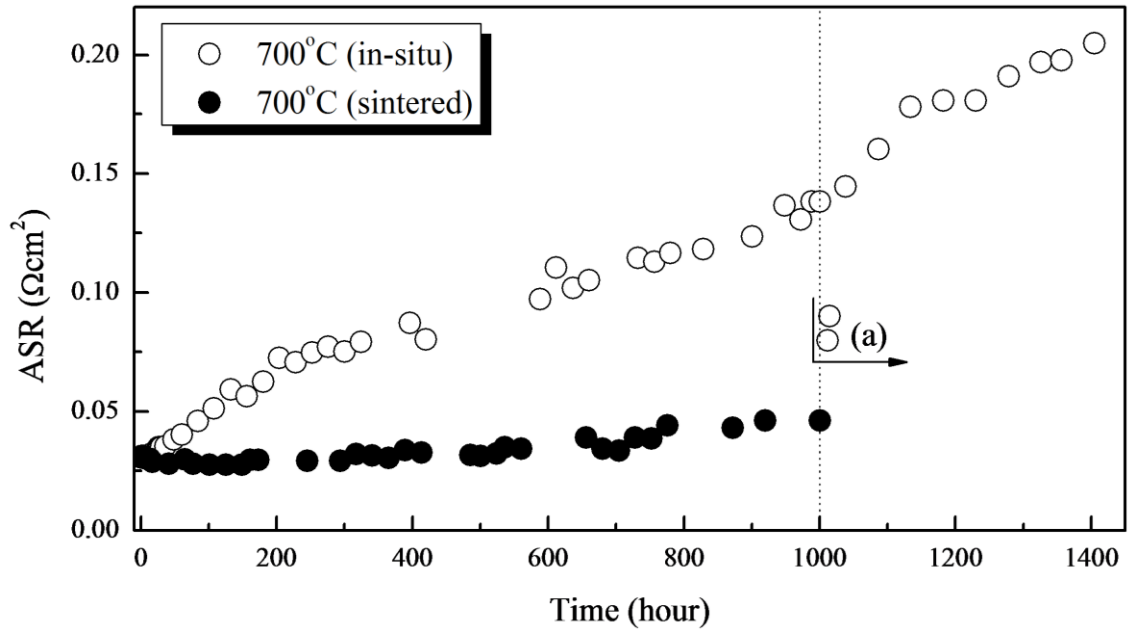


Fig. 1

Fig. 1. Area specific resistances (ASRs) of the SBSCO:50 cathode on top of a CGO91 electrolyte with respect to the measuring times. The results, displayed as black open circles, originate from the in-situ SBSCO:50 cathode; the closed circles indicate results coming from a sintered SBSCO:50 cathode. All results were measured at 700 °C.

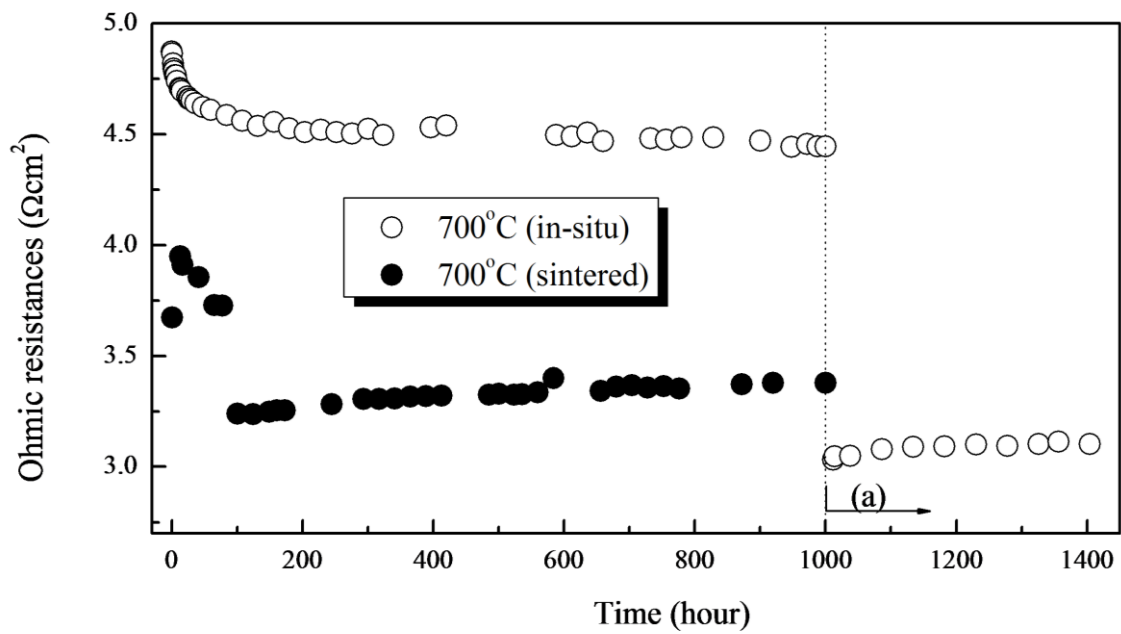


Fig. 2

Fig. 2. Ohmic resistances of the in-situ sample and of the sintered sample measured at 700 °C.



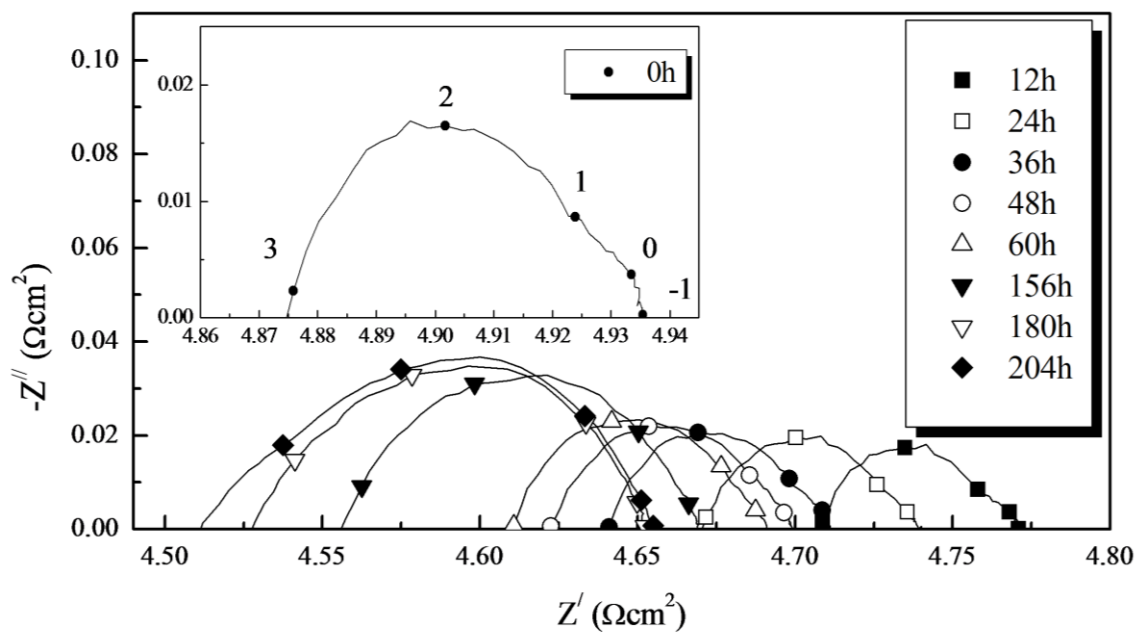


Fig. 3. (a)

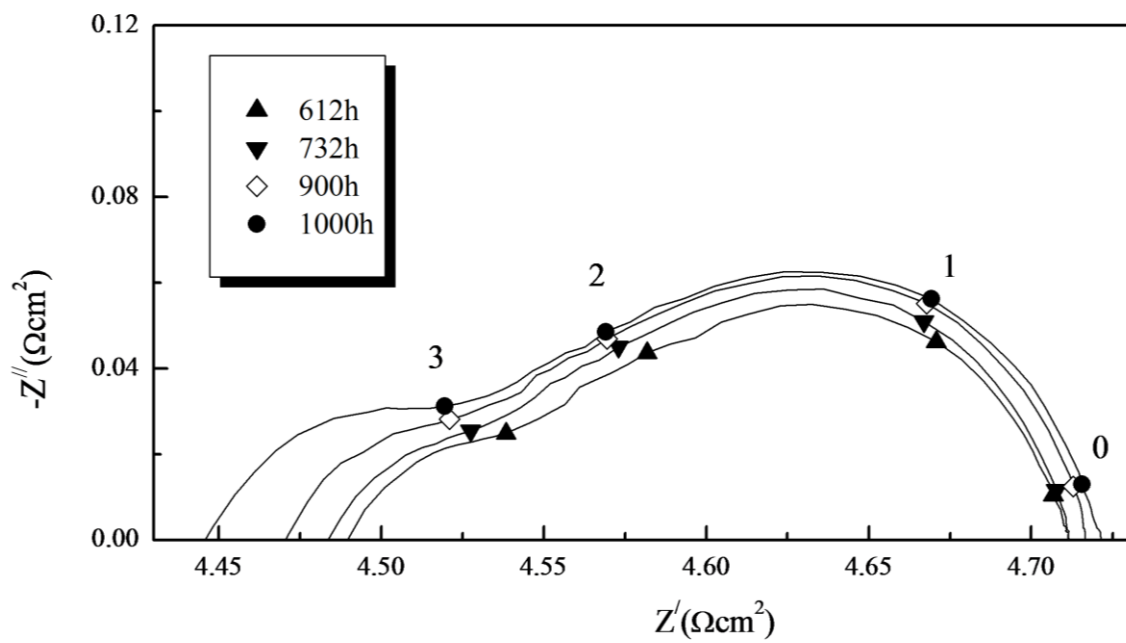


Fig. 3. (b)

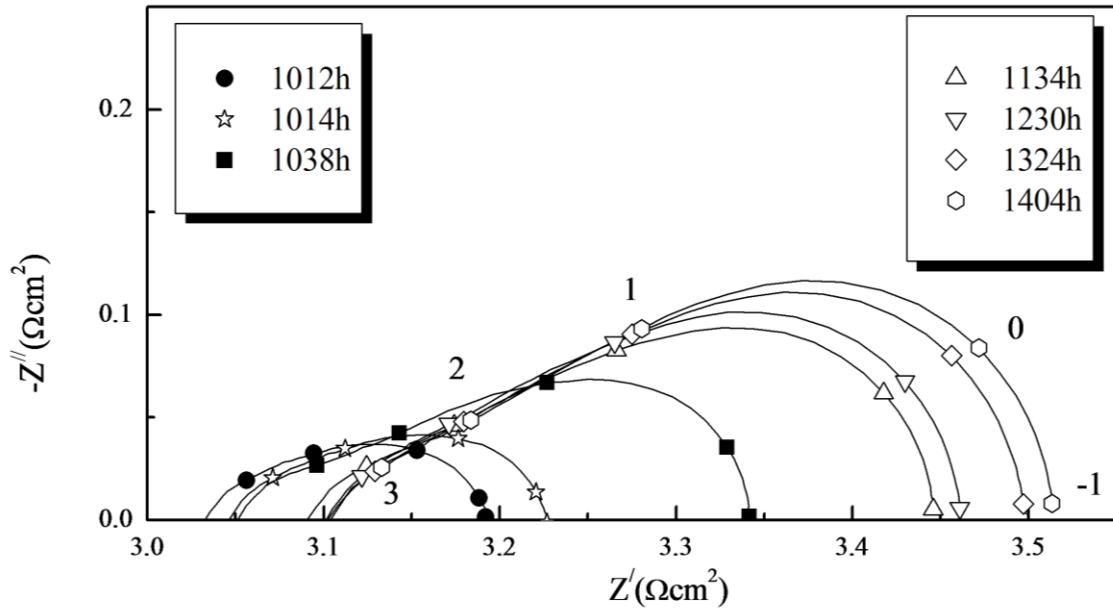


Fig. 3. (c)

Fig. 3. Impedance plots for the in-situ SBSCO:50 cathode on a CGO91 electrolyte measured at 700 °C. (a) and (b) show the impedance properties from the initial stage of measurement up to 1000 hours. (c) displays the impedance results for the in-situ cathode after sintering at 1000 °C for 1 hour.

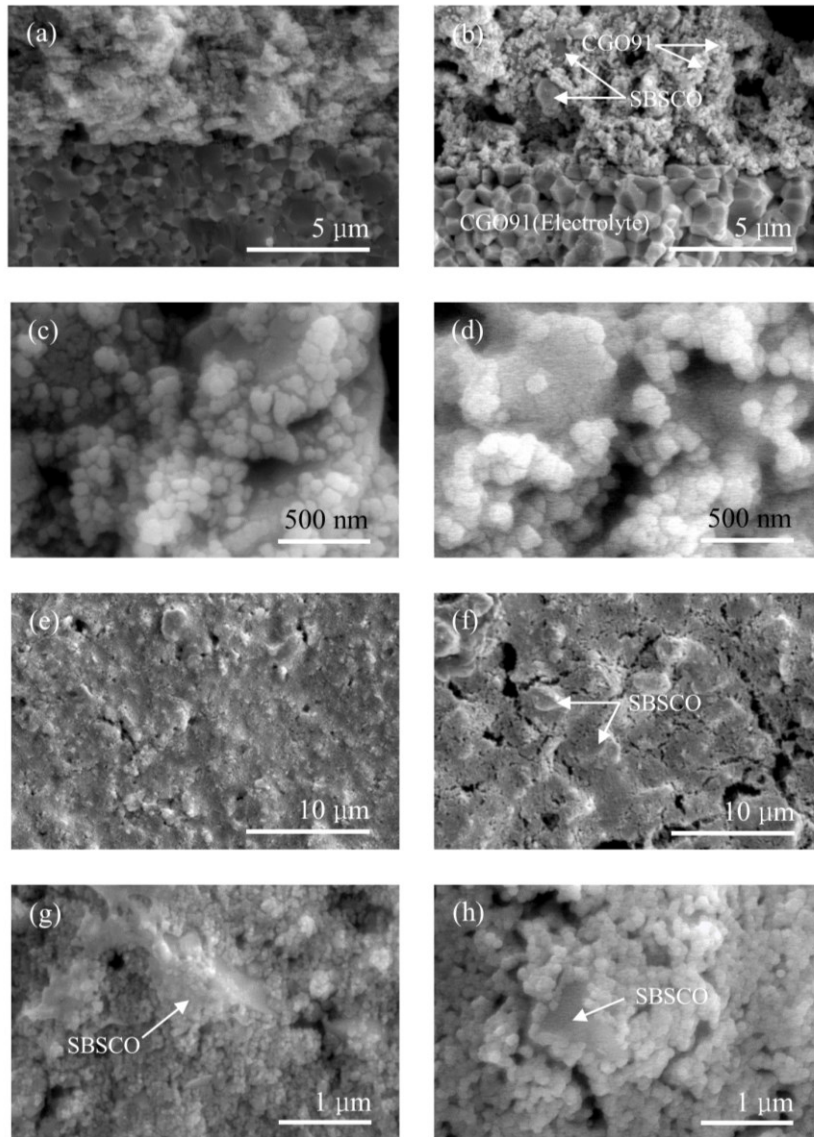


Fig. 4

Fig. 4. SEM images of the in-situ sample and of the sintered cathode. (a), (b), (c) and (d) are cross view images of the in-situ sample and of the sintered cathode. (e), (f), (g) and (h) are top view results. The sintered sample in this paper was sintered at 1000 °C for 1 hour. SBSCO was found to form 1~2 μm sized particles; the small sized particles consist of CGO91.

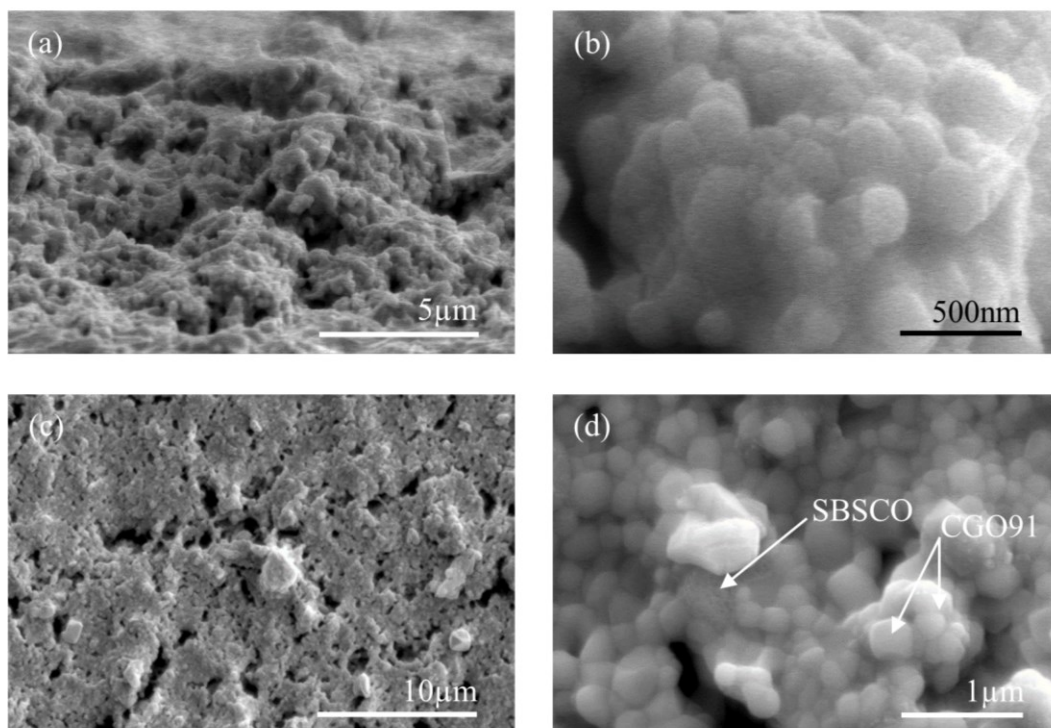


Fig. 5

Fig. 5. SEM images of the in-situ SBSCO:50 cathode after completion of sintering and of the long-term test. (a) and (b) are cross views and (c) and (d) are top views of the cathode. Significantly, this sample was sintered at 1000 °C for 1 hour after 1000 hours of measuring time.

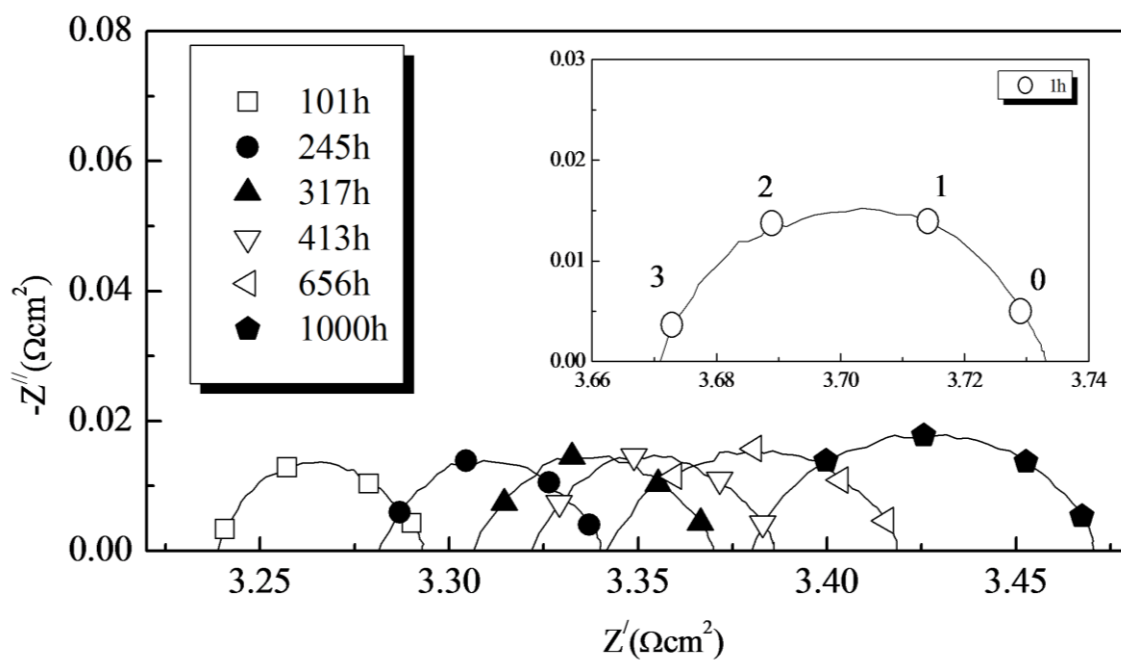


Fig. 6

Fig. 6. Impedance plots of a sample sintered at 1000 °C for 1 hour measured at various measuring times. The in-set numbers denote the logarithm of the measuring frequency.

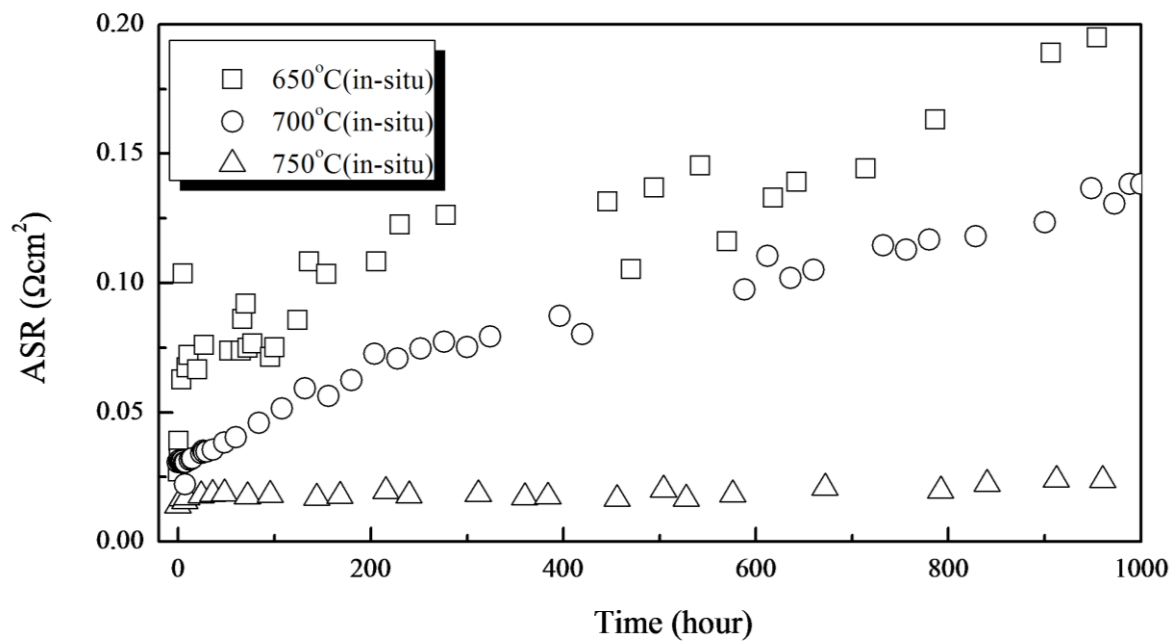


Fig. 7

Fig. 7. ASRs of the in-situ SBSCO cathode measured at various temperatures (650, 700 and 750 °C) for 1000 hours.

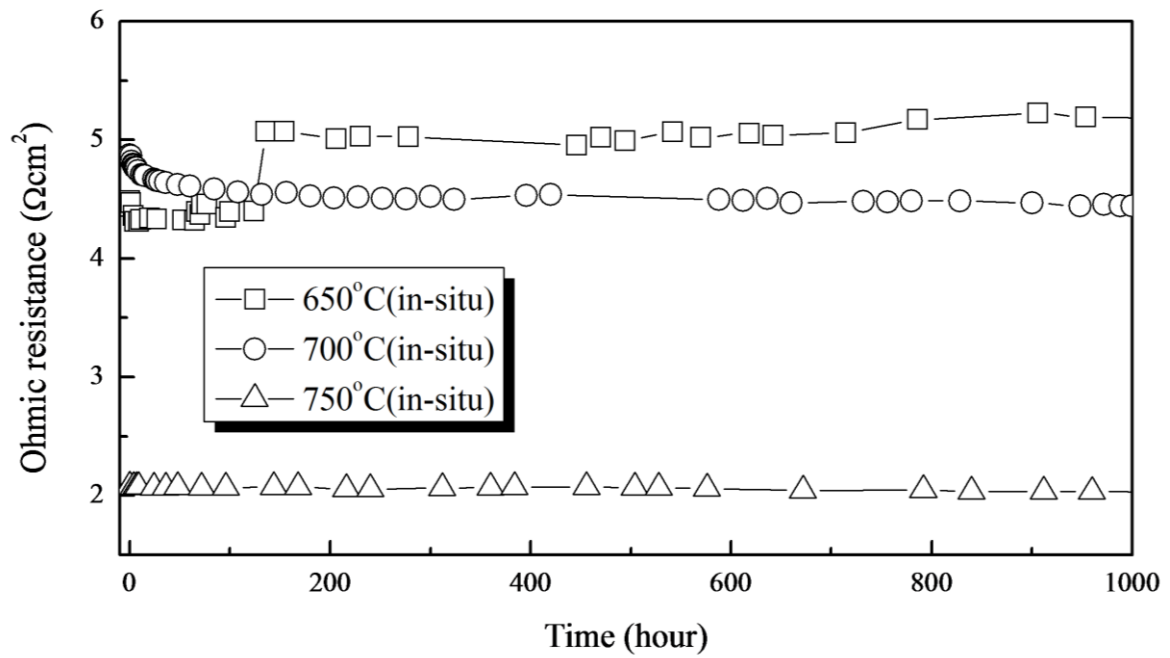


Fig. 8

Fig. 8. Ohmic resistances of the in-situ SBSCO:50 cathode sample measured at 650, 700 and 750 °C for 1000 hours. These results were extracted from the intercept of the high frequency part of the spectra with the  $Z'$  axes of the Nyquist plots.



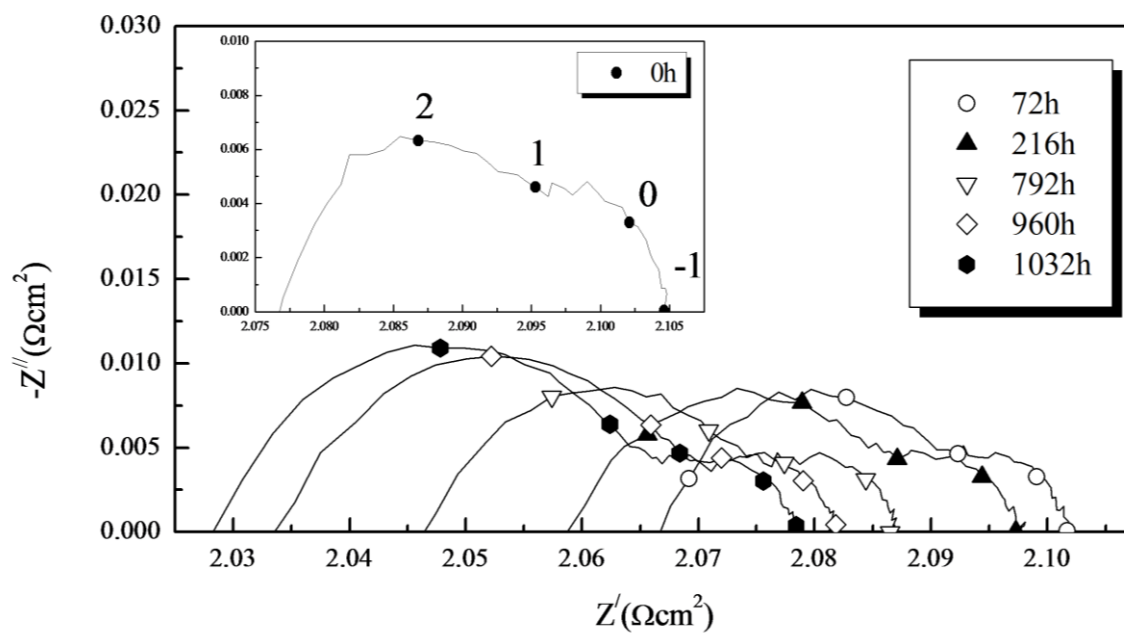


Fig. 9

Fig. 9. Impedance plots measured for the in-situ SBSCO:50 cathode at 750 °C. The inset numbers denote the logarithm of the measuring frequency.

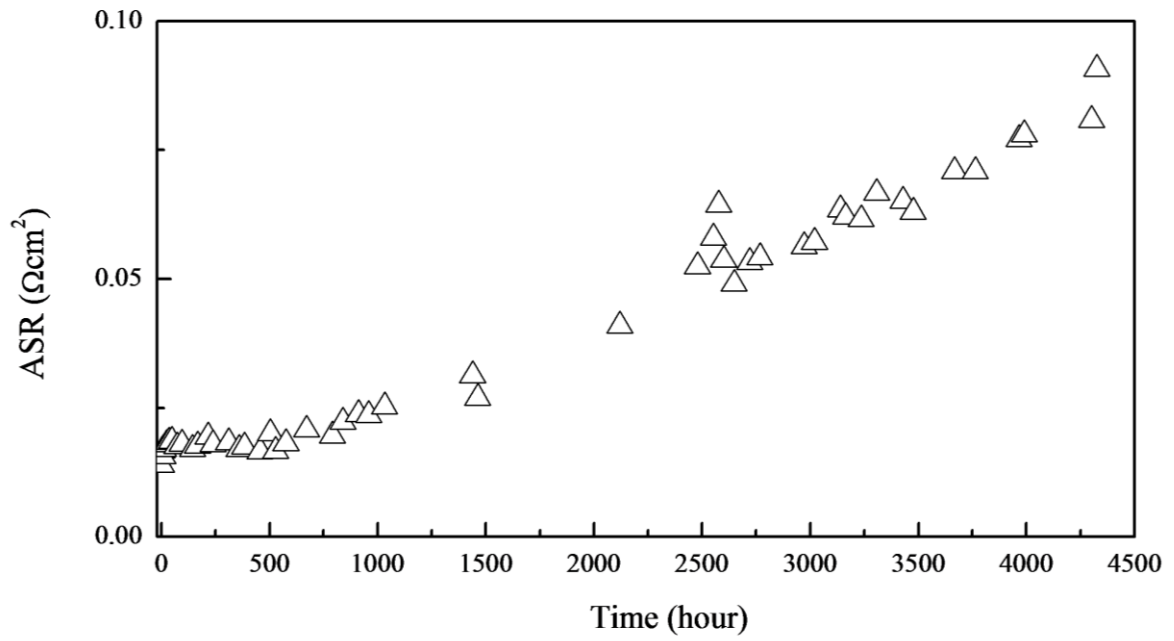


Fig. 10.

Fig. 10. Long term performance of the in-situ SBSCO:50 cathode extending the measuring time to 4300 hours at 750 °C.